Coupled dipole method to compute optical torque: Application to a micropropeller

Patrick C. Chaumet[a)]
Institut Fresnel (UMR 6133), Université Paul Cézanne, Avenue Escadrille Normandie-Niemen,
F-13397 Marseille cedex 20 France

C. Billaudeau
Laboratoire de Photonique et de Nanostructures (CNRS), Route de Nozay, F-91460 Marcoussis, France

The coupled dipole method is a volume integral equation method which allows computation of the scattered field from an arbitrary object (shape and relative permittivity). This method has been extended to the computation of optical forces. In this article we further extend the coupled dipole method to the computation of optical torque. First, we establish the equation to obtain the optical torque using the coupled dipole method, stressing the importance of the radiative reaction term. Second, we compare our theory to existing models for validation. Third, we apply our method to the computation of optical torque, from a plane wave circularly polarized on a micropropeller. The influence of geometry and relative permittivity on the optical torque is studied. © *2007 American Institute of Physics*. [DOI: 10.1063/1.2409490]

I. INTRODUCTION

Since the pioneering work by Ashkin and Gordon, it has been known that optical fields produce a net force on neutral particles.[1–3] Optical force has been extensively used in a wide range of applications: manipulation of particles through optical tweezers (theoretical[4–8] as well as experimental[9]), transport of neutral particles in a hollow waveguide[10] or Bose-Einstein condensates over large distances,[11] creation of microstructures by optical binding,[12–15] assembly of objects ranging from microspheres to biological cells,[16,17] and measures of van der Waals forces between a dielectric wall and an atom.[18] For a complete review on optical trapping see Refs. 19 and 20 and references therein.

The uses of these optical forces are not limited to transporting and manipulating particles; they can also be used to induce optical rotation, i.e., optical forces can create an optical torque. One of the first experiments was carried out by Higurashi *et al.* in 1994,[21] and Gauthier developed one of the first theoretical models in 1995.[22,23] More recently it has been shown that optical torque can be used for optically driven micromachines.[24–27] The computation methods in Refs. 22, 23, and 25–27 used a ray optics model. Yet, in the present article the size of the object under study is smaller than or of the order of the wavelength of illumination. In this case the ray optics model fails, and other methods must be used. Many theories allow a computation of optical torque on an arbitrary object. One can cite the *T*-matrix method,[28] the finite-difference time-domain (FDTD),[29] multipole *t*-matrix,[30] and more, generally all numerical methods rigorously based on electromagnetic theory.[31] Following the pioneering work of Draine,[32] we use the coupled dipole method (CDM), which is a volume-integral equation method. One advantage of this method is that it applies to arbitrarily

shaped, inhomogeneous, anisotropic particles. Hence very complex objects can be treated, such as a micropropeller, and the influence of its shape and the nature of its constituents can be studied in an efficient way. Also, the influence of the nature of the illumination, which can have unexpected effects,[33] can be studied. Moreover, the CDM permits the computation of the optical torque by taking into account both the "orbital" and "spin" optical angular momentum in an unified way. Furthermore, the computation is confined to the volume of the scatterer. One drawback is that computation time and memory requirements become difficult to manage when the particles are larger than the wavelength of illumination. Consequently, the CDM perfectly applies to computation of the optical torque of micro- and nano-objects.

In Sec. II A we develop the theory necessary to compute the optical torque from the CDM while stressing the importance of the radiative reaction term. In Sec. II B we give some details concerning the manner in which the computations are performed in order to optimize the computation time. In Sec. III A we validate the proposed method on an object of particular shape, and in Sec. III B we investigate the optical torque on a complex object which can be used as a micropropeller. The influence of geometry and relative permittivity on the optical torque is studied. Finally, we present our conclusion in Sec. IV.

II. COMPUTATION OF THE OPTICAL TORQUE

A. Theory

Recently, we presented an optical force computation method using the coupled dipole method (CDM).[34] Here, we will simply recall the main steps to obtain the optical force; then, we will concentrate on developing the computation of optical torque. The CDM is used to derive the local field

---

a)Electronic mail: patrick.chaumet@fresnel.fr

inside the object:[35] the object is discretized into N dipolar subunits and the local field at each subunit satisfies the following self-consistent equation:

$$\mathbf{E}(\mathbf{r}_i) = \mathbf{E}_0(\mathbf{r}_i) + \sum_{j=1, i \neq j}^{N} \mathbf{T}(\mathbf{r}_i, \mathbf{r}_j) \alpha(\mathbf{r}_j) \mathbf{E}(\mathbf{r}_j), \qquad (1)$$

where $\mathbf{E}_0$ is the incident field which illuminates the object, $\mathbf{T}$ is the linear response to a dipole in free space[36] (also called field susceptibility, which is proportional to free-space Green tensor), $\mathbf{p}(\mathbf{r}_i) = \alpha(\mathbf{r}_j)\mathbf{E}(\mathbf{r}_j)$ is the dipole moment of subunit j, where $\alpha(\mathbf{r}_j)$ is the dynamic polarizability of subunit j and is expressed as[37]

$$\alpha(\mathbf{r}_j) = \overline{\alpha}(\mathbf{r}_j)/[1 - (2/3)ik_0^3\overline{\alpha}(\mathbf{r}_j)]. \qquad (2)$$

Here, k_0 is the modulus of the wave vector of the incident wave, and $\overline{\alpha}(\mathbf{r}_j)$ contains the Clausius-Mossotti relation,

$$\overline{\alpha}(\mathbf{r}_j) = \frac{3d^3}{4\pi} \frac{\varepsilon(\mathbf{r}_j) - 1}{\varepsilon(\mathbf{r}_j) + 2}, \qquad (3)$$

where d is the lattice spacing of the discretization, and $\varepsilon(\mathbf{r}_j)$ the relative permittivity of subunit j, which is constant throughout the object if it is homogeneous. Note that if one wants to study an object which is birefringent, this characteristic is entered at this stage through $\varepsilon(\mathbf{r}_j)$, which becomes a tensor. The expression $\alpha(\mathbf{r}_j)$ relates to the fact that the field applied to subunit j is the scattered field from all other subunits plus the radiative reaction term, $\mathbf{E}_s(\mathbf{r}_j)$, which is the field from the subunit at its own location. This is written as $\mathbf{E}_s(\mathbf{r}_j) = i(2/3)k_0^3\mathbf{p}(\mathbf{r}_j)$.[37] Hence the dipole moment of subunit j reads as

$$\mathbf{p}(\mathbf{r}_j) = \overline{\alpha}(\mathbf{r}_j)[\mathbf{E}_s(\mathbf{r}_j) + \mathbf{E}(\mathbf{r}_j)] = \alpha(\mathbf{r}_j)\mathbf{E}(\mathbf{r}_j). \qquad (4)$$

With Eqs. (3) and (4) one can find the expression of $\alpha(\mathbf{r}_j)$ as in Eq. (2). For more details about the radiative reaction term see Refs. 38 and 39. To obtain the time-averaged optical force on each subunit, the derivative of the local field is required; therefore, we differentiate Eq. (1),[40]

$$\left(\frac{\partial \mathbf{E}(\mathbf{r})}{\partial u}\right)_{\mathbf{r}=\mathbf{r}_i} = \left(\frac{\partial \mathbf{E}_0(\mathbf{r})}{\partial u}\right)_{\mathbf{r}=\mathbf{r}_i}$$
$$+ \sum_{j=1, j \neq i}^{N} \left(\frac{\partial}{\partial u}\mathbf{T}(\mathbf{r}, \mathbf{r}_j)\right)_{\mathbf{r}=\mathbf{r}_i} \alpha(\mathbf{r}_j)\mathbf{E}(\mathbf{r}_j), \quad (5)$$

where u or v, stand for either x, y, or z. Once the local electric field and its derivative are known, the component of the total force on the ith subunit is given by[41]

$$F_u(\mathbf{r}_i) = \frac{1}{2}\text{Re}\left\{\sum_{v=1}^{3} p_v(\mathbf{r}_i)\frac{\partial[E^v(\mathbf{r}_i)]^*}{\partial u}\right\}, \qquad (6)$$

where * denotes the complex conjugate. To compute the force exerted by the light on any given object, one has to sum the forces experienced by each dipole composing the object.

We now want to compute the optical torque exerted on an object around a rotation axis Δ (Fig. 1). Hence the component of the optical torque we are interested in is along the Δ axis, due solely to the component of the perpendicular
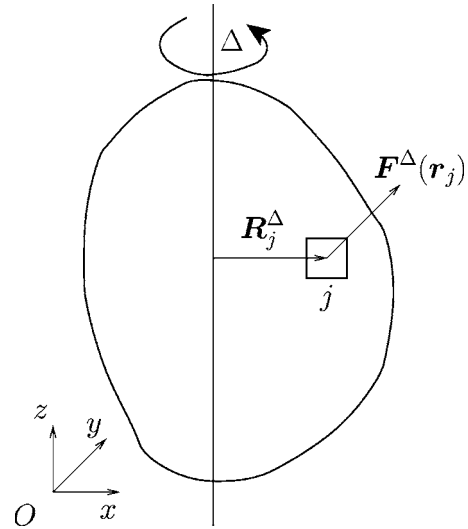

FIG. 1. Arbitrary object with a rotation axis of Δ. The square is an element of the discretization of the object. $\mathbf{R}_j^\Delta$ is the distance between subunit j and the rotation axis, and $\mathbf{F}^\Delta(\mathbf{r}_j)$ is the component of the optical force perpendicular to the axis Δ acting on subunit j.

force. Therefore, the superscript Δ in the equations means that only the component perpendicular to the Δ axis is taken into consideration. First, we compute the optical torque exerted on subunit j for the set of the subunit. In the *static case* it is easy to show that the optical torque exerted on a dipole $\mathcal{P}$, submitted to a electric static field $\mathcal{E}$, and to an external force $\mathcal{F}$, is given by $\Gamma = \mathbf{R}^\Delta \times \mathcal{F}^\Delta + \mathcal{P}^\Delta \times \mathcal{E}^\Delta$, where $\mathbf{R}^\Delta$ represents the position of the dipole relative to the Δ axis (Fig. 1). Our case is very similar; however, we should perform the time average, so the optical torque writes as

$$\Gamma(\mathbf{r}_j) = \mathbf{R}_j^\Delta \times \mathbf{F}^\Delta(\mathbf{r}_j) + \frac{1}{2}\text{Re}\{\mathbf{p}^\Delta(\mathbf{r}_j)$$
$$\times [\mathbf{E}^\Delta(\mathbf{r}_j) + \mathbf{E}_s^\Delta(\mathbf{r}_j)]^*\}. \qquad (7)$$

For an easier computation one can write Eq. (7), with Eq. (4), in the following form:

$$\Gamma(\mathbf{r}_j) = \mathbf{R}_j^\Delta \times \mathbf{F}^\Delta(\mathbf{r}_j) + \frac{1}{2}\text{Re}\{\mathbf{p}^\Delta(\mathbf{r}_j) \times [\mathbf{p}^\Delta(\mathbf{r}_j)/\overline{\alpha}(\mathbf{r}_j)]^*\}.$$
$$(8)$$

The first term of Eq. (8) is the optical torque due to the optical force [Eq. (6)] perpendicular to the Δ axis. As this term depends on the rotation axis, it is usually called the extrinsic part of the optical torque (or orbital angular momentum). The second term represents the optical torque due to the alignment of the dipole with the applied field at its location. This term does not depend on the choice of the rotation axis and it is usually called the intrinsic part of the optical torque (or spin angular momentum).[42] For further reading on optical angular momentum flow, refer to Ref. 43.

Remember that in the second part of Eq. (7), the field applied to subunit j is the sum of the fields scattered by all other subunits, $\mathbf{E}^\Delta(\mathbf{r}_j)$, plus the field due to the subunit itself, i.e., $\mathbf{E}_s^\Delta(\mathbf{r}_j)$. This term introduced in Eq. (4) respects the optical theorem, hence conserving the momentum. In Eq. (7) this term further allows the angular momentum to be con-

served. As an example, take a sphere that is small enough—compared to the wavelength of illumination—to be assimilated to a dipole. This sphere is illuminated by a circularly polarized plane wave which propagates along the Δ axis confounded with the z axis: for example $\mathbf{E}_0 = E_0(1,i,0)e^{ik_0z}$, which implies $\mathbf{p} = \alpha E_0(1,i,0)e^{ik_0z}$. In this case the optical force is restricted to the z axis; hence the optical torque writes as

$$\Gamma = \frac{1}{2}\mathrm{Re}[\mathbf{p}^\Delta \times (\mathbf{p}^\Delta/\overline{\alpha})^*] = E_0^2\frac{|\alpha|^2}{|\overline{\alpha}|^2}\mathrm{Im}(\overline{\alpha}) \qquad (9)$$

$$\approx E_0^2\,\mathrm{Im}(\overline{\alpha}). \qquad (10)$$

The approximation leading from Eq. (9) to Eq. (10) is possible since we assumed that the sphere is small compared to the wavelength of illumination. In the case of a lossless dielectric sphere (for which the polarizability $\overline{\alpha}$ is real) a well-known result appears: the sphere cannot rotate under a circularly polarized plane wave.[44,45] In the case of an absorbing sphere the optical torque is proportional to the imaginary part of its polarizability. This is coherent with the fact that the optical torque of an absorbing sphere is proportional to its absorbing cross section,[46] which in turn is proportional to $\mathrm{Im}(\overline{\alpha})$ in the case of a small particle.[46,47] Note that the sphere's sense of rotation depends on the polarization of the incident wave (left-handed or right-handed).

There is some difference between our Eq. (8) and that used in the pioneering work of Draine.[32] First, his optical torque was not computed around a rotation axis, and second he omitted the radiative reaction term, $\mathbf{E}_s^\Delta$, in Eq. (8) in computing the optical torque. This omission was of little consequence on the results presented by Draine, as the relative permittivity of the object under study had a strong imaginary part. In the case of a lossless sphere, however, its omission would create an optical torque in contradiction with the result of Watermann[44] [for example, Eq. (10) becomes $\Gamma = E_0^2\,\mathrm{Im}(\alpha) \neq 0$].

In conclusion, with the CDM the total optical force exerted on an object and the total optical torque around an axis Δ writes as

$$\mathbf{F} = \sum_{j=1}^{N} \mathbf{F}(\mathbf{r}_j), \qquad (11)$$

$$\Gamma = \sum_{j=1}^{N} \Gamma(\mathbf{r}_j), \qquad (12)$$

where $\mathbf{F}(\mathbf{r}_j)$ and $\Gamma(\mathbf{r}_j)$ are obtained from Eqs. (6) and (8), respectively.

B. Some details on the numerical computation

As stated in the Introduction, the computation time can become difficult to manage when the particle size increases. The linear system represented by Eq. (1) can be rewritten in a more condensed form as
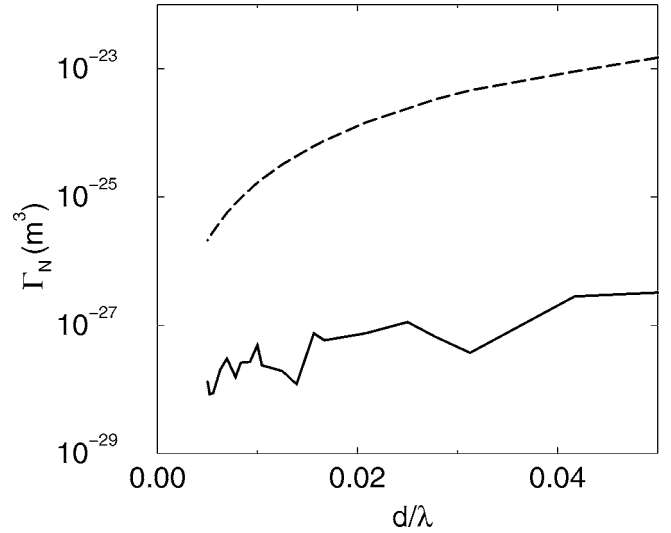

FIG. 2. Study of the normalized optical torque vs d/λ on a dielectric sphere ($\varepsilon = 2.25$) with radius $a = \lambda/4$ illuminated by a circularly polarized plane wave. Solid line the optical torque is computed in using Eq. (7), and dashed line without taking into account the radiative reaction term in Eq. (7).

$$(\mathbf{I} - \mathbf{A}\boldsymbol{\alpha})\mathbf{E} = \mathbf{E}_0, \qquad (13)$$

where $\mathbf{I}$, $\mathbf{A}$, and $\boldsymbol{\alpha}$ are $3N \times 3N$ matrices. $\mathbf{I}$ is the identity matrix, $\boldsymbol{\alpha}$ a diagonal matrix which contains the polarizabilities, and $\mathbf{A}$ a matrix which contains all the tensor $\mathbf{T}(\mathbf{r}_i,\mathbf{r}_j)$. The field $\mathbf{E}$ is found by solving the linear system of Eq. (13) iteratively using the quasiminimal residual method of Freund and Nachtigal,[48] to avoid the inversion of the matrix $(\mathbf{I} - \mathbf{A}\boldsymbol{\alpha})$. Notice that the product $\mathbf{A}\boldsymbol{\alpha}\mathbf{E}$ is performed with the fast Fourier transform with $\mathbf{A}$ as a Toeplitz matrix. One can also write the sum of Eq. (5) as a convolution product. Hence, we can still use the fast Fourier transform to decrease the time of computation of this sum.[40]

III. RESULTS

A. Particular case of a sphere and an ellipsoid

To validate the model, we first studied the cases of particular shape such as a sphere or an ellipsoid. In Fig. 2 we present the optical torque normalized to $4\pi\varepsilon_0|E_0|^2$: $\Gamma_N = \Gamma/(4\pi\varepsilon_0|E_0|^2)$ (notice that in this article we will present always the normalized optical torque which is in m^{-3}) for a sphere illuminated by a plane wave, more particularly a right-handed circularly polarized wave, which propagates along the z axis: $\mathbf{E}_0 = E_0(1,\,i,\,0)e^{ik_0z}$.[49] The radius of the sphere is $a = \lambda/4$ and the relative permittivity is such that $\varepsilon = 2.25$. We remark that when experimenting with optical torque, the object under study is often embedded in a liquid medium. In this case ε is the ratio between the relative permittivity of the object and the relative permittivity of the liquid. Figure 2 shows the optical torque versus d/λ when we use Eq. (7) (solid line) and when the radiative reaction term is omitted in Eq. (7) (dashed line). When we use Eq. (7) the optical torque vanishes, but due to numerical errors it is not exactly zero and we have some oscillations. The dashed line shows that when the radiative reaction term is not used in Eq. (7), first the optical torque is nonzero, and second, the
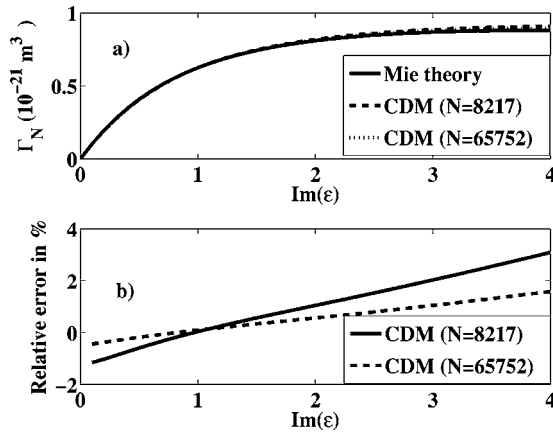
FIG. 3. Study of the normalized optical torque on a sphere with radius $a=\lambda/4$ illuminated by a circularly polarized plane wave. (a) Optical torque vs Im(ε) [Re(ε)=2.25] obtained from the Mie series (plain line), and the CDM: $N=8217$ (dashed line), and $N=65752$ (dotted line). (b) Relative error in percent for optical torque obtained from the Mie series and from the CDM.

optical torque depends on the discretization. This shows the importance of taking the radiative reaction term into account, in this case.

In Fig. 3 we present the optical torque with the same condition of illumination as those used in Fig. 2. The radius of the sphere is $a=\lambda/4$ and the relative permittivity is such that Re(ε)=2.25. Figure 3(a) shows the optical torque plotted versus the imaginary part of the relative permittivity. The curves with dashed and dotted lines are computed with the CDM for different values of N. The curve with a plain line is obtained from Eqs. (7), (8), and (36) taken from Ref. 46, which shows that the optical torque for a sphere illuminated by a circularly polarized plane wave can be expressed as

$$\Gamma = \frac{E_0^2}{4\pi k_0} C_{\text{abs}}, \tag{14}$$

where C_{abs} is the absorbing cross section which can be obtained from the Mie series [for a small sphere compared to the wavelength $C_{\text{abs}}=4\pi k_0 \, \text{Im}(\bar{\alpha})$]. One can notice that the curve obtained with $N=65\,752$ is superposed with the optical torque obtained from Eq. (14). Figure 3(b) shows the relative error in percent between the results obtained from Eq. (14) and the CDM. With $N=65\,752$ the relative error remains below the 2% level. To improve the convergence a recent improvement to the CDM should be applied.[40,50] We have checked that, if the radiative reaction term is not taken into account in Eq. (7), the curve obtained in that case is no different than those obtained with the rigorous computation. This is due to the absorbing part of the relative permittivity as stated in Sec. II A.

Next, we illuminated an ellipsoid (ε=2.25) defined by $[(x/2)^2+y^2+z^2]<\lambda/4(N=28\,256)$, hence twice as wide in the x direction as along the y and z axis. The illumination is a plane wave where the electric field forms an angle of φ with the x axis: $\mathbf{E}_0=E_0[\cos(\varphi), \sin(\varphi), 0]e^{ik_0z}$ (see the inset of Fig. 4). Figure 4 shows the optical torque versus φ. The optical torque vanishes 4 times, showing that elongated particles tend to align along their long and short axes, but the
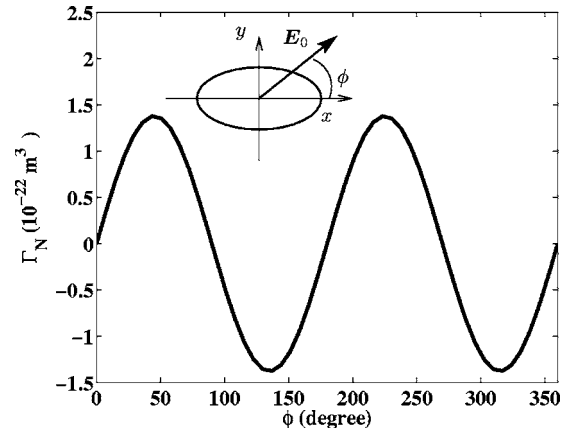

FIG. 4. Normalized optical torque vs ϕ the angle between the x axis and $\mathbf{E}_0$. The object is an ellipsoid wider in the direction of x, see inset.

equilibrium is stable only along the long axes. This effect has been observed experimentally on nanorods.[51] This can be explained by the small size of the particle compared to the wavelength: from Eq. (8) the optical torque is expressed as $\Gamma \approx E_0^2 \sin(2\varphi)(\bar{\alpha}_{xx}-\bar{\alpha}_{yy})/4$, where the polarizability of an ellipsoid can be deduced from Ref. 52. Hence, the optical torque vanishes when $\sin(2\varphi)=0$. Notice that particles which have different polarizabilities along their short and long axes act as if they were birefringent[28] as the optical torque also depends on $\sin(2\varphi)=0$ for a birefringent object under a linearly polarized wave.[53]

B. Micropropeller

Recent technological progress has made it possible to design complex objects of micrometer size, and to build micromotors set into motion by light; see for example Ref. 24. The rotation of this micropropeller is often explained by analogy with the wind on the vanes of a windmill.[24] Hence, it would be interesting to study the effect of the shape and the relative permittivity on such micropropellers. For this, we chose a simplified micropropeller (see Fig. 5), although it is possible to study more complex objects with the CDM. The angle between the vanes and the x axis is α, and the rotation axis Δ is the z axis. For the sake of simplicity, the
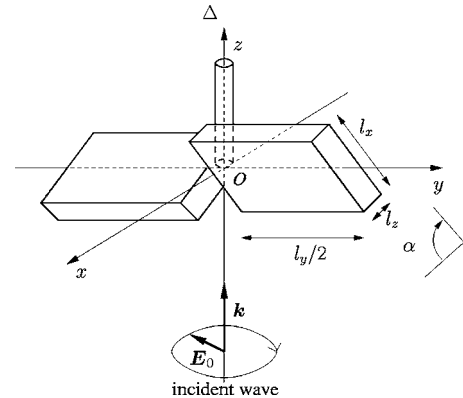

FIG. 5. The object under study is a micropropeller illuminated by a right-handed circularly polarized wave which propagates along the z axis: $\mathbf{E}_0=E_0(1, i, 0)e^{ik_0z}$. The angle between the two vanes and the x axis is α.
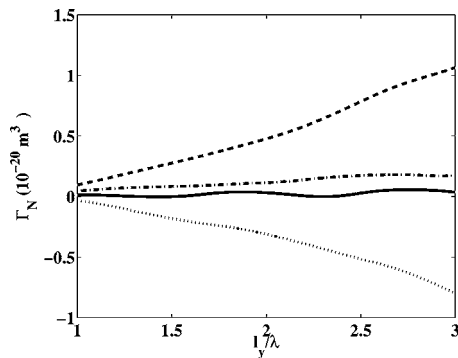
FIG. 6. The object under study is a micropropeller (Fig. 5) illuminated by a circularly polarized plane wave. The normalized optical torque is plotted vs l_y with $l_x=0.8\lambda$, $l_z=0.4\lambda$ for different angles α: $\alpha=0°$ in plain line, $\alpha=60°$ in dashed line, $\alpha=90°$ in dot-dashed line, and $\alpha=-60°$ in dotted line.

rotation axis of the micropropeller (cylinder along the z axis in Fig. 5) is not taken into account in the computation of the optical torque.

Note that in our study we investigated a micropropeller of the same size as the wavelength of illumination.

If the illumination is linearly polarized, the micropropeller tends to align its long and short axes in the electric field (using the same explanation as previously seen for the ellipsoid), and there is no micropropeller rotation. This problem is circumvented by illuminating the object with a right-handed circularly polarized wave which propagates along the z axis: $\mathbf{E}_0=E_0(1, i, 0)e^{ik_0z}$ ($E_0=1$ for Figs. 6 and 7; see Fig. 5).

1. Influence of the geometry

First, we studied the effect of micropropeller geometry on the optical torque. Figure 6 represents the effect of vane length (l_y) and angle α of the vane with $l_x=0.8\lambda$ and $l_z=0.4\lambda$, and $\varepsilon=2.25$ (as micropropellers are always studied in a liquid environment ε corresponds to the contrast in relative permittivity of the object and the liquid).

In fact, when $\alpha=0°$ (plain line) and $\alpha=90°$ (dot-dashed line) we have a parallelepiped; thus, the optical torque is due only to the transfer of angular momentum from the incident wave to the micropropeller. If the parallelepiped were small
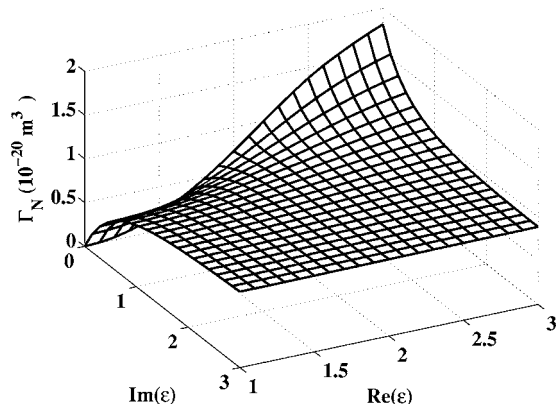

FIG. 7. The object under study is a micropropeller (Fig. 5) illuminated by a circularly polarized plane wave. The normalized optical torque is plotted vs Re(ε) and Im(ε) with $l_x=0.8\lambda$, $l_y=3.0\lambda$, $l_z=0.4\lambda$, and $\alpha=60°$.

enough compared to the wavelength, the optical torque could be written, from Eq. (8), as $\Gamma=(1/3)E_0^2k_0^3(\overline{\alpha}_{xx}-\overline{\alpha}_{yy})^2$. Hence, the greater the difference between the dimensions l_x and l_y, the stronger the optical torque. In our opinion, this explains why optical torque is stronger when $\alpha=90°$ than when $\alpha=0°$. When l_y increases the optical torque presents some oscillations. In our opinion these oscillations are produced by geometrical resonance and are particularly strong when $\alpha=0°$, where the optical torque can be either positive or negative.

The maximum optical torque is obtained for $\alpha=60°$ plotted as a dashed line. When l_y increases, the optical torque increases more or less linearly. If $\alpha=-60°$ the optical torque becomes negative, but the absolute value is smaller than when $\alpha=60°$. This is due to the incident plane wave which is polarized to the right. Thus, we can divide the optical torque into two parts: one due to the circular polarization of the incident wave (which gives, e.g., the optical torque on an ellipsoid) and the other due to the geometry of the micropropeller (angle of the vane). In order to optimize the optical torque (as far as possible) these two parts should contribute to give an optical torque with the same sign, which is the case for $\alpha=60°$.

Notice that the best α value yielding the strongest optical torque depends on the geometry of the micropropeller, i.e., l_x and l_z. For example with the previous l_x, ($l_x=0.8\lambda$), but with $l_z=0.2\lambda$ or $l_z=0.8\lambda$, the largest optical torque is obtained for $\alpha=50°$ and $\alpha=25°$, respectively. When l_x is larger, i.e., $l_z=0.4\lambda$ and $l_x=1.2\lambda$, the optical torque is larger for $\alpha=65°$.

2. Influence of the relative permittivity

Figure 7 shows the influence of the relative permittivity on the optical torque with the following geometry: $l_x=0.8\lambda$, $l_y=3.0\lambda$, $l_z=0.4\lambda$, and $\alpha=60°$.

From Fig. 7 it is obvious that the relative permittivity influences optical torque. However, the exact behavior is far from being trivial. For instance Fig. 7 shows that optical torque increases or decreases versus Im(ε) according to the value of Re(ε). With a different micropropeller geometry (change of l_x, l_y, and l_z) the behavior can be different. The only general behavior that we have observed is that an increase in Re(ε) always produces an increase in optical torque, regardless of the value of Im(ε) or the geometry of the micropropeller. In conclusion, it is difficult to predict which relative permittivity will optimize the optical torque.

Notice that if we take an irradiance of 20 mW/μm^2 ($4\pi\varepsilon_0|E_0|^2=1675$ kg m^{-1} s^{-2}), $\varepsilon=1.3$, which is typically used in experimentation,[24] Fig. 7 yields an optical torque of about $\Gamma=6.0\times10^{-19}$ N m. Our optical torque is about 100 times weaker that those in Ref. 24; however, our micropropeller is smaller and has only two arms.

IV. CONCLUSION

In conclusion, we have presented a method to compute optical torque using the coupled dipole method. We have shown that the radiative reaction term must be taken into account to express the optical torque on a dipolar subunit. We further validated our method with specific cases, and

showed that the CDM can be used to compute the optical torque on a complex object, which in this article is a micropropeller. We show that in this case it is difficult to predict the influence of the various parameters (angle of the vane, relative permittivity) on the optical torque. Therefore, an experiment should begin with a theoretical study aimed at optimizing the micropropeller, for which the CDM is a perfectly adapted tool when the object is smaller or comparable to the wavelength of illumination. Notice that angular speed depends on the optical torque exerted by the light on the micropropeller, but also on the viscous drag force, which is difficult to evaluate in the case of complex shapes.

The theory presented in this article can easily be extended to an object upon a flat substrate.[34] Note that the optical torque experiment uses more complex beams such as Laguerre-Gauss modes,[54] optical vortices[55] which can easily be included in the CDM through the incident field $\mathbf{E}_0$ in Eq. (1).

[1] A. Ashkin, Phys. Rev. Lett. **24**, 156 (1970).

[2] A. Ashkin, Phys. Rev. Lett. **25**, 1321 (1970).

[3] J. P. Gordon, Phys. Rev. A **8**, 14 (1973).

[4] L. Novotny, R. X. Bian, and X. S. Xie, Phys. Rev. Lett. **79**, 645 (1997).

[5] K. Okamoto and S. Kawata, Phys. Rev. Lett. **83**, 4534 (1999).

[6] P. C. Chaumet, A. Rahmani, and M. Nieto-Vesperinas, Phys. Rev. Lett. **88**, 123601 (2002).

[7] P. C. Chaumet, A. Rahmani, and M. Nieto-Vesperinas, Phys. Rev. B **66**, 195405 (2002).

[8] P. C. Chaumet, A. Rahmani, and M. Nieto-Vesperinas, Phys. Rev. B **71**, 045425 (2005).

[9] A. Ashkin, J. M. Dziedzic, J. E. Bjorkholm, and S. Chu, Opt. Lett. **11**, 288 (1986).

[10] R. Gómez-Medina, A. García-Martín, M. Lester, M. Nieto-Vesperinas, and J. J. Sáenz, Phys. Rev. Lett. **86**, 4275 (2001).

[11] T. L. Gustavson, A. P. Chikkatur, A. E. Leanhardt, A. Görlitz, S. Gupta, D. E. Pritchard, and W. Ketterle, Phys. Rev. Lett. **88**, 020401 (2001).

[12] M. I. Antonoyiannakis and J. B. Pendry, Phys. Rev. B **60**, 2363 (1999).

[13] M. M. Burns, J.-M. Fournier, and J. A. Golovchenko, Phys. Rev. Lett. **63**, 1233 (1989).

[14] P. C. Chaumet and M. Nieto-Vesperinas, Phys. Rev. B **64**, 035422 (2001).

[15] R. Gómez-Medina and J. J. Sáenz, Phys. Rev. Lett. **93**, 243602 (2004).

[16] R. Holmlin, M. Schiavoni, C. Chen, S. Smith, M. Prentiss, and G. Whitesides, Angew. Chem., Int. Ed. **39**, 3503 (2000); E. R. Dufresne, G. C. Spalding, M. T. Dearing, S. A. Sheets, and D. G. Grier, Rev. Sci. Instrum. **72**, 1810 (2001); E. R. Dufresne and D. G. Grier, *ibid.* **69**, 1974 (1998).

[17] M. P. Macdonald, L. Paterson, K. Volke-Sepulveda, J. Arlt, W. Sibbet, and K. Dholakia, Science **296**, 1101 (2002).

[18] A. Landragin, J.-Y. Courtois, G. Labeyrie, N. Vansteenkiste, C. I. Westbrook, and A. Aspect, Phys. Rev. Lett. **77**, 1464 (1996).

[19] K. C. Neuman and S. M. Block, Rev. Sci. Instrum. **75**, 2787 (2004).

[20] D. G. Grier, Nature **424**, 810 (2003).

[21] E. Higurashi, H. Ukita, H. Tanaka, and O. Ohguchi, Appl. Phys. Lett. **64**, 2209 (1994).

[22] R. C. Gauthier, Appl. Phys. Lett. **67**, 2269 (1995).

[23] R. C. Gauthier, Appl. Phys. Lett. **69**, 2015 (1996).

[24] P. Galajda and P. Ormos, Appl. Phys. Lett. **78**, 249 (2001).

[25] M. E. J. Friese, H. Rubinsztein-Dunlop, J. Gold, P. Hagberg, and D. Hanstorp, Appl. Phys. Lett. **78**, 547 (2001).

[26] R. C. Gauthier, R. N. Tait, and M. Ubriaco, Appl. Opt. **41**, 2361 (2002).

[27] H. Ukita and K. Nagatomi, Appl. Opt. **42**, 2708 (2003).

[28] A. I. Bishop, T. A. Nieminen, N. R. Heckenberg, and H. Rubinsztein-Dunlop, Phys. Rev. A **68**, 033802 (2003).

[29] W. L. Collett, C. A. Ventrice, and S. Mahajan, Appl. Phys. Lett. **82**, 2730 (2003).

[30] F. J. Garcìa de Abajo, J. Quant. Spectrosc. Radiat. Transf. **89**, 3 (2004).

[31] F. M. Kahnert, J. Quant. Spectrosc. Radiat. Transf. **79–80**, 775 (2003).

[32] B. T. Draine and J. C. Weingartner, Astrophys. J. **470**, 551 (1996).

[33] P. Galajda and P. Ormos, Appl. Phys. Lett. **80**, 4653 (2002).

[34] P. C. Chaumet and M. Nieto-Vesperinas, Phys. Rev. B **61**, 14119 (2000); **62**, 11185 (2000).

[35] E. M. Purcell and C. R. Pennypacker, Astrophys. J. **186**, 705 (1973).

[36] J. D. Jackson, *Classical Electrodynamics*, 2nd ed. (Wiley, New York, 1975), p. 395.

[37] B. T. Draine, Astrophys. J. **333**, 848 (1988).

[38] P. C. Chaumet, A. Sentenac, and A. Rahmani, Phys. Rev. E **70**, 036606 (2004).

[39] P. C. Chaumet, Appl. Opt. **43**, 1825 (2004).

[40] P. C. Chaumet, A. Rahmani, A. Sentenac, and G. W. Bryant, Phys. Rev. E **72**, 046708 (2005).

[41] P. C. Chaumet and M. Nieto-Vesperinas, Opt. Lett. **25**, 1065 (2000).

[42] C. Cohen-Tanoudji, J. Dupont-Roc, and G. Grynberg, *Processus d'Interaction entre Photons et Atomes* (InterEdition, Paris, 1988).

[43] S. M. Barnett, J. Opt. B: Quantum Semiclassical Opt. **4**, S7 (2002).

[44] P. C. Waterman, Phys. Rev. D **3**, 825 (1971).

[45] I. A. Nieminen, Opt. Commun. **235**, 227 (2004).

[46] P. L. Marston and J. H. Crichton, Phys. Rev. A **30**, 2508 (1984).

[47] S. Chang and S. S. Lee, J. Opt. Soc. Am. B **2**, 1853 (1985).

[48] R. W. Freund and N. M. Nachtigal, Numer. Math. **60**, 315 (1991).

[49] The definition of the right handed polarized electric wave is defined as in M. Born and E. Wolf, *Principles of Optics* (Pergamon, London, 1959), p. 29.

[50] A. Rahmani, P. C. Chaumet, and G. W. Bryant, Astrophys. J. **607**, 873 (2004).

[51] K. D. Bonin, B. Kourmanov, and T. G. Walker, Opt. Express **10**, 984 (2002).

[52] J. A. Stratton, *Electromagnetic Theory* (McGraw-Hill, New York, 1941).

[53] A. La Porta and M. D. Wang, Phys. Rev. Lett. **92**, 190801 (2004).

[54] S. J. Parkin, T. A. Nieminen, N. R. Heckenberg, and H. Rubinsztein-Dunlop, Phys. Rev. A **70**, 023816 (2004).

[55] N. R. Heckenberg, M. E. J. Friese, T. A. Nieminen, and H. Rubinsztein-Dunlop, in *Optical Vortices*, edited by M. Vasnetsov and K. Staliunas (Nova Science Publishers, Hauppauge, NY, 1999), Chap. 3, pp. 75–105.